JOURNAL OF SOLID STATE CHEMISTRY 87, 134–140 (1990)

Synthesis, Crystal Structure, and Physical Properties of Sr_2N

NATHANIEL E. BRESE AND MICHAEL O'KEEFFE[1]

Department of Chemistry, Arizona State University, Tempe, Arizona 85287

Received November 29, 1989

Sr_2N has been synthesized from the elements and its structure determined by time-of-flight neutron diffraction. Crystal data: $R\bar{3}m$, $a = 3.8566(1)$ Å, $c = 20.6958(4)$ Å, $V = 266.58(1)$ Å^3, $Z = 3$, $D_x = 2.13$, $T = 300$ K, $R_{wp} = 0.077$, $R_p = 0.056$, reduced $\chi^2 = 2.06$ for 25,368 profile points and 53 variables. Sr_2N crystallizes with the layered $CdCl_2$ structure as formerly proposed. N atoms center flattened octahedra with six equal N–Sr distances of 2.6118(3) Å. The Sr–Sr distances in the octahedral layer are 3.8566(1) ($6x$) and 3.523(1) ($3x$). The Sr–Sr distances between layers are 4.726(1). It has been argued that Sr_2N is actually $Sr_2N_xH_y$; but the neutron data show the absence of any hydrogen contamination. Sr_2N is a metallic conductor with a weak temperature-independent paramagnetism.

Introduction

The crystal chemistry of the alkaline earth nitrides is remarkable. One expects a simple stoichiometry of M_3N_2 for all alkaline earth nitrides. This is indeed observed for Be_3N_2 and Mg_3N_2; both crystallize with the anti-bixbyite (cubic Mn_2O_3) structure (*4–6*), although Be_3N_2 heated in the presence of Si also forms a high-temperature polymorph based on hexagonal packing (*7*). The normal, brown calcium nitride (Ca_3N_2) also forms with the anti-bixbyite structure (*8, 9*), although black hexagonal Ca_3N_2 (*10*), yellow orthorhombic Ca_3N_2 (*10*), reddish-brown tetragonal $Ca_{11}N_8$ (*11*), greenish-black hexagonal Ca_2N (anti-$CdCl_2$) (*12*), and CaN (*13*) (which is likely the imide CaNH (*14*)) are also reported. That a compound of composition Ba_3N_2 has been synthesized is confirmed only by chemical analysis (*15–17*). The X-ray powder patterns could not be indexed (*18, 19*); the indexing on a hexagonal cell by Linke and Lingmann (*20*) is questionable as their data do not correspond to those collected by previous workers or by us. Ca_2NH, Sr_2NH, and Ba_2NH all crystallize with a superstructure of rock salt (*21–23*).

Three black nitrides have been reported to crystallize from Sr metal. SrN was reported to have the rock salt structure (*24*). A composition of Sr_3N_2 was deduced from elemental analysis (*15, 16, 25*), and a Debye–Scherrer pattern was collected (*26*) and indexed on a centered monoclinic cell (*27*). The structure of Sr_2N was determined to be anti-$CdCl_2$ using single-crystal X-ray diffraction data (*1*).

Gaudé and Lang later declared that "Sr_3N_2" was actually a mixture of SrN and Sr_2N (*28*). Motte (*29*) stated that "Sr_3N_2" was actually $Sr_3N_{2-x}Hy$ which could be indexed on the same centered monoclinic cell

[1] To whom correspondence should be addressed.

0022-4596/90 $3.00

reported by Gaudé *et al.* Brice claimed (*2*) that Sr_2N was actually $Sr_3N_{2-x}H_y$ or Sr_2NH_x ($0.4 < x < 1$) and that SrN is actually $SrN_{1-x}H_x \cdot nSrO$ ($0.02 < n < 0.08$). He further claimed that Sr_3N_2 will never form if even small traces of H are present. His only evidence was (reportedly quite precise) chemical analysis (*2*). Hydrogen dissolved in the starting Sr was blamed for its presence, and a leaky apparatus was blamed for the oxygen contamination. Hulliger also questions the existence of the alkaline earth nitrides M_2N since they are reportedly not metallic conductors (*3*).

We designed a very clean system for the preparation of nitrides and followed the course of reaction by a technique we call "thermobarometric analysis" (TBA). Analysis for the presence of H was by examination of the background of a neutron diffraction pattern which is very sensitive to the presence of ^1H.

Experimental

Synthesis

An Al_2O_3 jacket (Coors porcelain) was soaked in nitric acid, rinsed repeatedly with deionized water, and heated to 900°C under flowing oxygen then vacuum (10^{-3} Torr). A quartz tube was cleaned thoroughly in an acid solution (HF/HNO_3), rinsed repeatedly with distilled water, and heated to 900°C under air and then under vacuum (10^{-3} Torr). The jacket and tube (still under vacuum) were passed into an Ar-filled glovebox. The white oxide coating from a Sr rod of 3 cm diameter (Johnson Matthey, 99+%) was filed off, and fresh Sr filings were loaded into the Al_2O_3 jacket which was itself placed in the quartz tube. The assembly was attached to a stopcock, passed out of the drybox, and evacuated to better than 10^{-5} Torr. Nitrogen, purified over Dow Q-5 catalyst (Vacuum Atmospheres) to ppb levels of contamination, was introduced into the vacuum line to a total pressure of 100 Torr. All valves were closed except those to a pressure gauge and the sample. The pressure remained static (to better than 0.1 mTorr) for over a day. The temperature was slowly increased to 750°C, although reaction began below 300°C as shown by a gradual drop in pressure. The stoichiometry derived from the pressure change in the calibrated volume and the known amount of sample is $Sr_{2.01(2)}N$. Figure 1 shows the pressure drop as a function of temperature for a typical preparation.

A second TBA experiment was conducted using our Sr_2N neutron sample as the starting material. Deuterium gas was introduced into the line. No pressure drop was observed until 400°C (very rapid reaction at 470°C); the Sr_2N was converted to a mixture of approximately equal amounts of SrND and SrD_2. Mass spectral analysis on the residual gases revealed only excess D_2 gas. We conclude that hydrogen is not present in "all reported Sr_2N," as claimed by Brice, and further that it is not a very favorable reaction. Studies are underway to intercalate halides into the Sr_2N gap.

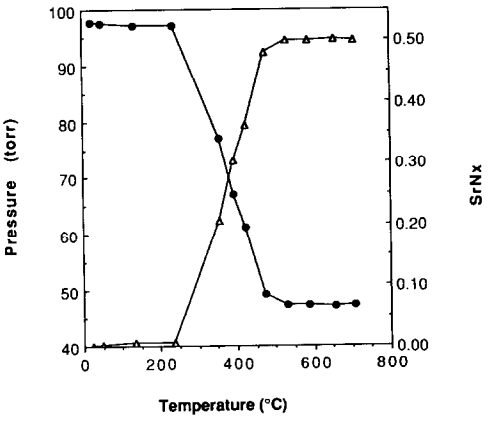

FIG. 1. Pressure and composition as a function of temperature for a typical thermobarometric analysis experiment. Data points are not equilibrium values.

Structural Study

The purity of the Sr metal and of the products was assessed on a Rigaku D/Max-IIB X-ray powder diffractometer. Pulsed neutron diffraction data were collected at room temperature on the Neutron Powder Diffractometer (NPD) of the Manuel Lujan, Jr. Neutron Scattering Center at Los Alamos National Laboratory. The powder data were refined with use of the General Structure Analysis System (GSAS), a Rietveld profile analysis code (*30*). Data employed were collected from the $2\theta = \pm 148°$ and $\pm 90°$ detector banks. The final refinement included 375 reflections in the range $0.48\ \text{Å} < d < 3.0\ \text{Å}$ (5961 profile points) for the back-scattering detector banks and 358 reflections in the range $0.48\ \text{Å} < d < 3.6\ \text{Å}$ (6723 profile points) for the 90° banks. The 53 variables refined included 24 background coefficients (6 for each bank) used in a cosine Fourier series technique, an absorption factor for each $\pm\theta$ bank (*31, 32*), a profile coefficient for each bank (σ_1) (*33*), diffractometer zero constants, lattice parameters, an atomic position parameter, and anisotropic thermal parameters. Also included in the final refinement were variables (σ_2^2, σ_{2e}^2) to model the anisotropic particle-size broadening along [001]. The small "anthills" in the difference profile for the 001 reflections are inadequately modeled by our profile functions. Apparently the material crystallizes with strain exhibited as Lorentzian broadening (i.e., broad bases). The final conventional agreement indices are $R_p = 0.056$ and $R_{wp} = 0.078$ with a reduced $\chi^2 = 2.06$. An analysis of agreement factors versus parity class revealed no unusual trends.

The highest feature on a difference Fourier map was 1.7% the height of an N atom (the strongest neutron scatterer). As a check on our model, we tried (separately) to refine the occupancy of N, Sr, and H in three likely positions in the van der Waals gap (one-, two-, and three-coordinated to the Sr atoms with appropriate bond length constraints); the Sr and N occupancies remained at unity, and all H atoms fractions refined to zero or negative occupancy.

It seems unlikely that enough hydrogen could be absorbed in the Sr metal to cause such great levels of claimed contamination (e.g., up to 1 H atom per 3 Sr atoms for $Sr_2NH_{0.63}$). Clearly these large amounts of hydrogen claimed would have to be stored (at least partially) as SrH_2. Since the structures of Sr and SrH_2 are dramatically different (cubic vs orthorhombic), we calculated X-ray patterns using the program LAZY-PULVERIX (*34*), and they appear very different. All the lines on our experimental X-ray powder patterns of the starting material could be accounted for as arising from pure Sr.

Since ^1H has an extremely large incoherent neutron cross section (81.5 barns versus 7.6 for deuterium (*35*)), its presence in a sample is very apparent if one examines the background of a neutron diffraction pattern. Experts visually estimated that there could not be more than at most a few percent ^1H in the sample (*36*). This, the lack of evidence for H in the starting materials, and the featureless difference map lead us to conclude that there is no H in the van der Waals gap of Sr_2N as previously claimed.

Figure 2 shows the final Rietveld refinement profile fit for the $-90°$ data. Atomic positions and anisotropic thermal parameters are given in Tables I and II, respectively. Structure amplitudes are given in Table III.[1]

[1] See NAPS document No. 04774 for 17 pages of supplementary material. Order from ASIS/NAPS. Microfiche Publications, P.O. Box 3513, Grand Central Station, New York, NY 10163. Remit in Advance $4.00 for microfiche copy or for photocopy, $7.75 up to 20 pages plus $0.30 for each additional page. All orders must be prepaid. Institutions and Organizations may order by purchase order. However, there is a billing and handling charge for this service of $15. Foreign orders add $4.50 for postage and handling, for the first 20 pages, and $1.00 for additional 10 pages of material, $1.50 for postage of any microfiche orders.

TABLE I

POSITIONAL PARAMETERS[a] FOR Sr_2N

Atom	Site	x	y	z	100 U_{eqv}[b]
Sr	6c	0	0	0.26737(3)	1.43
N	3a	0	0	0	1.47

[a] Spacegroup $R\bar{3}m$, a = 3.8566(1) Å, c = 20.6958(4) Å (Hexagonal Cell), a = 7.2490(5) Å, α = 30.853(1)° (rhombohedral cell).

[b] U_{eqv} is $\frac{1}{3}$ the trace of the matrix of temperature factors.

TABLE II

ANISOTROPIC THERMAL PARAMETERS FOR Sr_2N[a]

Atom	U_{11}	U_{33}	U_{12}
Sr	1.29(3)	2.34(5)	0.65(1)
N	0.90(3)	3.07(6)	0.45(1)

[a] All values to be multiplied by 10^{-2} Å^2. $U_{11} = U_{22}$; $U_{13} = U_{23} = 0$.

Physical Properties

Magnetic measurements were made on a SQUID magnetometer from the SHE Corporation. A small powdered sample (0.079 g) was loaded in a dry box into a Teflon container machined to accept a screw lid. The sample was quickly transferred to the He atmosphere of the magnetometer. Measurements were made from 0.05 to 3.0 T at 5 and 100 K. Measurements versus temperature were made at 0.1 T from 5–360 K. A blank run yielded the bucket correction; correction for the ion-core diamagnetism was also made (*37*). An X-ray pattern collected on this sample after the magnetic measurements was identical to that collected previously (i.e., pure Sr_2N).

SrN is reported to exhibit temperature-independent paramagnetism with χ of

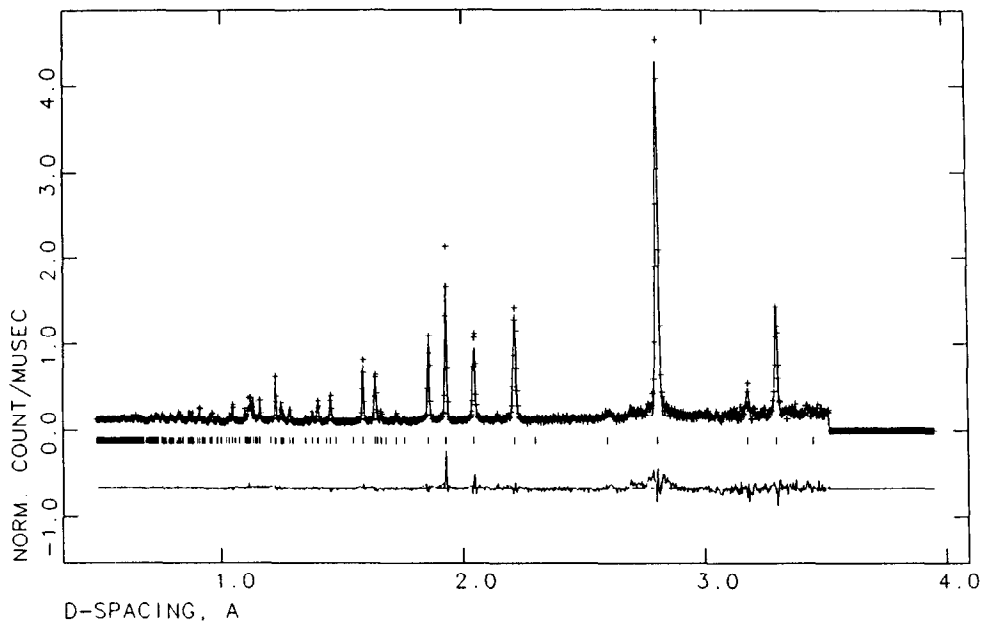

FIG. 2. Neutron diffraction profile fit for Sr_2N. The data points are shown as "+" and the solid line is the calculated profile. The difference curve at the bottom is on the same scale.

1.15×10^{-6} emu/g (*24*). Ariya and co-workers used the Gouy method to determine that Sr_2N also exhibits temperature-independent paramagnetic behavior with χ of 0.8×10^{-6} emu/g at 293 K (*38*). We confirm this behavior but find that the molar magnetic susceptibility at 300 K and 0.1 T is larger (1.35×10^{-3} emu/mole or 7.1×10^{-6} emu/g). The temperature dependence and magnitude of the susceptibility is characteristic of Pauli paramagnetism of conduction electrons. This agrees with conductivity measurements which indicate that Sr_2N is a metallic conductor. Gaudé reported a room-temperature conductivity of 500 Sm^{-1} (*1*). Our measurements on the compressed powdered neutron sample indicate σ(300 K) of 6000 Sm^{-1} and show that it decreases with increasing temperature as is typical of metallic conductivity.

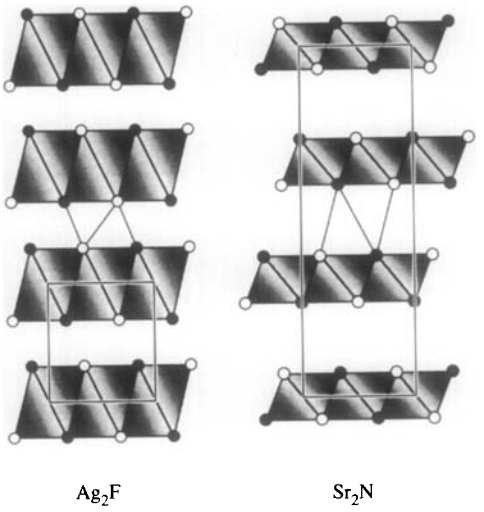

FIG. 3. Projections of the structures of Sr_2N (right) and Ag_2F (left) comparing the relative dimensions of the octahedra. The unit cell outlined is an orthohexagonal cell with c vertical and $a + b$ horizontal. Solid and empty circles represent metal atoms at $1/2\,(a + b)$ and $0\,(a + b)$, respectively. The nonmetal atoms center the shaded octahedra. One empty octahedron is outlined in each case.

Discussion

Sr_2N crystallizes with the layered $CdCl_2$ structure. Edge-sharing Sr octahedra make up slabs 2.73 Å thick with 4.17 Å gaps between them. The N atom is on a center of symmetry, so the six Sr–N bond lengths are equivalent (2.6118(3) Å). However, the coordination does distort somewhat from the ideal. The supplementary Sr–N–Sr bond angles are 84.83(2)° and 95.17(2)°.

The Sr–Sr distances are indicative of the irregularity of the octahedron. Each Sr atom has six Sr neighbors within the base of a slab (3.8566(1) Å) and three closer neighbors across the octahedron (3.523(1) Å). The Sr–Sr distances across the "van der Waals" gap are 4.726(1).

Silver subfluoride, Ag_2F, is diamagnetic, becomes a superconductor at low temperatures (*39*), and has the CdI_2 structure (*40*). This structure differs from that of Sr_2N in the stacking of the slabs. The two compounds would be isoelectronic were it not for the filled $4d^{10}$ shell of Ag, so a comparison of the two compounds is of interest. The FAg_6 octahedra, however, are *elongated* along the [001] direction, while the NSr_6 octahedra are *compressed*. Figure 3 shows a projection of the Sr_2N and Ag_2F structures for comparison. The short distance between the layers in Ag_2F is attributed to metal–metal bonding, while the great distances (0.42 Å greater than in Sr metal) between the corresponding layers in Sr_2N suggest short range repulsions that are counterbalanced by van der Waals attractions.

Using the bond-valence method of analysis (*41–43*), we find that the Sr atom appears to have an unsatisfied coordination sphere ($\Sigma v_{Sr-i} = 1.224$). The bond valence sum should be equal to its atomic valence. This leads to one of two conclusions. Either there are more atoms bonded to Sr atoms (e.g., H atoms in the van der Waals gap which the diffraction data rule out) than our model in-

cludes, or the bond-valence parameters used are not appropriate for Sr and N in unconventional valence states (e.g., $Sr^{+1.5}$ is different than Sr^{+2} to N^{-3}). We favor the latter description, since the valence sum at the N atom is also low ($\Sigma v_i = 2.45$). In addition, no features of a difference Fourier map suggested anything in the van der Waals gap.

We made Madelung potential calculations (assuming nonoverlapping spherical ions). With the formal valences $Sr^{1.5+}$ and N^{-3}, the calculated site potentials are -15.8 and 21.9 V, respectively. If we use more conventional valences of Sr^{2+} and N^{3-} neutralized by a uniformly distributed negative charge, we obtain site potentials of -21.4 and 21.5 V. Using a correlation that we have found between potentials at cation sites and bond-valence parameters (*44*), we expect a potential at the Sr site for a valence z of $-10.3z$ V, i.e., -15.5 or -20.6 V for $Sr^{1.5+}$ and Sr^{2+}, respectively. Both hypotheses for the formal valence of Sr are therefore equally likely on this basis.

Acknowledgments

This material is based upon work supported under a National Science Foundation Graduate Fellowship to N.E.B. and is part of a continuing program in crystal chemistry supported by the National Science Foundation (DMR 8813524). We have benefitted from the use of facilities at the Manuel Lujan, Jr. Neutron Scattering Center, a national user facility, funded as such, by the DOE/Office of Basic Energy Sciences. We thank G. Burr and R. B. Von Dreele for assistance with the neutron data collection. We thank B. L. Ramakrishna for his help with the magnetic measurements. The X-ray data were obtained on equipment purchased under National Science Foundation Grant DMR-8406823.

References

1. J. Gaudé, P. L'Haridon, Y. Laurent, and J. Lang, *Bull. Soc. Fr. Mineral. Cristallogr.* **95,** 56 (1972).
2. J.-F. Brice, J.-P. Motte, and J. Aubry, *Rev. Chim. Minér.* **12,** 105 (1975).
3. F. Hulliger, "Structural Chemistry of Layer-type Phases" (F. Lévy, Ed.), Reidel, Dordrecht (1976).
4. M. Von Stackelberg and R. Paulus, *Z. Phys. Chem. B* **22,** 305 (1933).
5. J. David, Y. Laurent, and J. Lang, *Bull. Soc. Fr. Minér. Cristallogr.* **94,** 340 (1971).
6. J. David, *Rev. Chim. Minér.* **9,** 717 (1972).
7. P. Eckerlin and A. Rabenau, *Z. Anorg. Allg. Chem.* **304,** 218 (1960).
8. Y. Laurent, *Rev. Chim. Minér.* **5,** 1019 (1968).
9. Y. Laurent, J. Lang, and M. T. Le Bihan, *Acta Crystallogr. B* **24,** 494 (1968).
10. Y. Laurent, J. David, and J. Lang, *C.R. Séances Acad. Sci. Ser. C* **259,** 1132 (1964).
11. Y. Laurent, J. Lang, and M. T. Le Bihan, *Acta Crystallogr. B* **25,** 199 (1969).
12. E. T. Keve and A. C. Skapski, *Inorg. Chem.* **7,** 1157 (1968).
13. P. Dutoit and A. Schnorf, *Compt. Rend.* **187,** 300 (1928).
14. H. Hartmann, H. J. Fröhlich, and F. Ebert, *Z. Anorg. Allg. Chem.* **218,** 181 (1934).
15. A. Guntz and F. Benoit, *Ann. Chim.* **20,** 5 (1923).
16. A. von Antropoff and K. H. Krüger, *Z. Phys. Chem. A* **167,** 49 (1933).
17. Y. Okamoto and J. C. Goswami, *Inorg. Chem.* **5,** 1281 (1966).
18. K. Torkar and H. T. Spath, *Monatsh. Chem.* **98,** 2020 (1967).
19. J. Gaudé and J. Lang, *C.R. Séances Acad. Sci. Ser. C* **274,** 521 (1972).
20. K.-H. Linke and H. Lingmann, *Z. Anorg. Allg. Chem.* **366,** 82 (1969).
21. J.-F. Brice, J.-P. Motte, and J. Aubry, *C.R. Séances Acad. Sci. Ser. C* **274,** 2166 (1972).
22. J.-F. Brice, J.-P. Motte, and J. Aubry, *C.R. Séances Acad. Sci. Ser. C* **276,** 1093 (1973).
23. J.-F. Brice, J.-P. Motte, A. Courtois, J. Protas, and J. Aubry, *J. Solid State Chem.* **17,** 135 (1976).
24. J. Gaudé, P. L'Haridon, Y. Laurent, and J. Lang, *Rev. Chim. Minér.* **8,** 287 (1971).
25. J. Gaudé and J. Lang, *C.R. Séances Acad. Sci. Ser. C* **271,** 510 (1970).
26. H.-H. Emons, D. Anders, G. Roewer, and F. Vogt, *Z. Anorg. Allg. Chem.* **333,** 99 (1964).
27. J. Gaudé and J. Lang, *Rev. Chim. Minér.* **7,** 1059 (1970).
28. J. Gaudé and J. Lang, *Rev. Chim. Minér.* **9,** 799 (1972).
29. J.-P. Motte, J.-F. Brice, and J. Aubry, *C.R. Séances Acad. Sci. Ser. C* **274,** 1814 (1972).
30. A. C. Larson and R. B. Von Dreele, Generalized Structure Analysis System, LANSCE, MS-H805, Manuel Lujan Neutron Scattering Center, Los Alamos, NM 87545, (1989).

31. K. D. ROUSE, M. J. COOPER, AND A. CHAKERA, *Acta Crystallogr. A* **26,** 682 (1970).
32. A. W. HEWAT, *Acta Crystallogr. A* **35,** 248 (1979).
33. R. B. VON DREELE, J. D. JORGENSEN, AND C. G. WINDSOR, *J. Appl. Crystallogr.* **15,** 581 (1982).
34. K. YVON, W. JEITSCHKO, AND E. PARTHÉ, Laboratoire de Cristallographie aux Rayons-X, Univ. de Geneva, 24 Quai Ernest Ansermet, CH 1211 Geneva 4, Switzerland, 1977.
35. "International Tables for X-ray Crystallography," Vol IV, Table 2.6, Kynoch Press, Birmingham (1974).
36. R. B. VON DREELE, personal communication (1989).
37. P. W. SELWOOD, "Magnetochemistry," 2nd ed., Interscience, New York (1956).
38. S. M. ARIYA, M. S. EROFEEVA, AND G. P. MACHALOY, *J. Gen. Chem. USSR* **27,** 1806 (1957).
39. K. ANDRES, N. A. KUEBLER, AND M. B. ROBIN, *J. Phys. Chem. Solids* **27,** 1747 (1966).
40. G. ARGAY AND I. NÁRAY-SZABÓ, *Acta Chim. Acad. Sci. Hung.* **49,** 329 (1966).
41. I. D. BROWN AND D. ALTERMATT, *Acta Crystallogr. B* **41,** 244 (1985).
42. M. O'KEEFE, *Struct. Bond.* **71,** 161 (1988).
43. N. E. BRESE AND M. O'KEEFFE, manuscript in preparation.
44. N. E. BRESE AND M. O'KEEFFE, manuscript in preparation.